Full Paper Transactions, SMiRT 28
Toronto, Canada, August 10-15, 2025

RATIONALIZATION OF SEISMIC RESPONSE ANALYSIS WITH BASEMAT－BOTTOM ADHESION FOR NUCLEAR POWER PLANT BUILDINGS

Takaki Tojo[1], Toshiya Miura[2], Noriki Nakai[3], Naohiko Tsunashima[4], Takuya Suzuki[5] and Naoto Yabushita[6]

[1] Senior researcher, R&D Institute, Takenaka Corporation, Chiba, Japan (toujou.takaki@takenaka.co.jp)
[2] Office of Civil Engineering and Architecture, Kansai Electric Power Company, Osaka, Japan (miura.toshiya@e5.kepco.co.jp)
[3] Leader, Office of Civil Engineering and Architecture, Kansai Electric Power Company, Osaka, Japan (nakai.noriki@b5.kepco.co.jp)
[4] Manager, Office of Civil Engineering and Architecture, Kansai Electric Power Company, Osaka, Japan (tsunashima.naohiko@e3.kepco.co.jp)
[5] Senior Chief Researcher, R&D Institute, Takenaka Corporation, Chiba, Japan (suzuki.takuya@takenaka.co.jp)
[6] Group Leader, Power Engineering, Engineering Division, Takenaka Corporation, Tokyo, Japan (yabushita.naoto@takenaka.co.jp)

ABSTRACT

Seismic response analysis that considers basemat uplift is crucial for the seismic design of critical buildings within nuclear power plants. This study assesses the impact of basemat bottom adhesion on the seismic response of these vital structures by utilizing a three-dimensional finite element model (3D FEM). The investigation focused on determining the effective magnitude of adhesion to prevent basemat uplift across different building weights and ground conditions. The finite element analysis results revealed that a minimum ground contact ratio of 35% or higher, without adhesion, could be enhanced with the inclusion of adhesion, indicating uplift suppression. Additionally, to streamline the analytical evaluation process involving adhesion, a comparison was made between the minimum contact ratios obtained from the 3D FEM and a previously established simplified method to examine the applicability of the simplified method. The simplified method effectively evaluated the impact of adhesion on minimum contact ratios for ground contact ratios of 35% or higher, with and without adhesion and seismic responses in the horizontal direction.

INTRODUCTION

Seismic response analysis that considers basemat uplift is required for the seismic design of critical buildings for nuclear power plants. The reduction in ground contact ratio caused by basemat uplift can lead to excessive responses in both the foundation and superstructure. In buildings on bedrock, adhesion between the bedrock and basemat can be expected. Adhesion can suppress seismic responses. However, the degree of adhesion varies, depending on the soil characteristics of the construction site (e.g., Tanaka et al., 2007). Therefore, understanding the range of effective adhesion that impacts seismic responses is crucial. The evaluation procedure for the analysis is shown in Figure 1, considering the basemat uplift in the current seismic design technical code (Japan Electric Association, 2021). When assessing basemat uplift behavior with a ground contact ratio below 50%, a detailed examination is required. Specifically, seismic response analysis using a three-dimensional finite element model for ground modeling (3D soil FEM) is employed when considering the impacts of adhesion. While previous studies suggest that the ground contact ratio of 3D soil FEM is limited to approximately 35% (Japan Electric Association, 2021), this approach significantly increases the computational cost of the analysis.

This study utilized 3D soil FEM to assess the seismic response characteristics related to basemat uplift under varying ground conditions, building weights, and adhesion levels, focusing on the correlation between building weight and adhesion.

Furthermore, while previous simplified methods that consider existing adhesion are computationally efficient, their applicability range has not been thoroughly examined. To validate the simplified method, a comparison was made between the response analysis results obtained using the simplified method and a 3D soil FEM, with the latter considered as a more detailed solution approach.

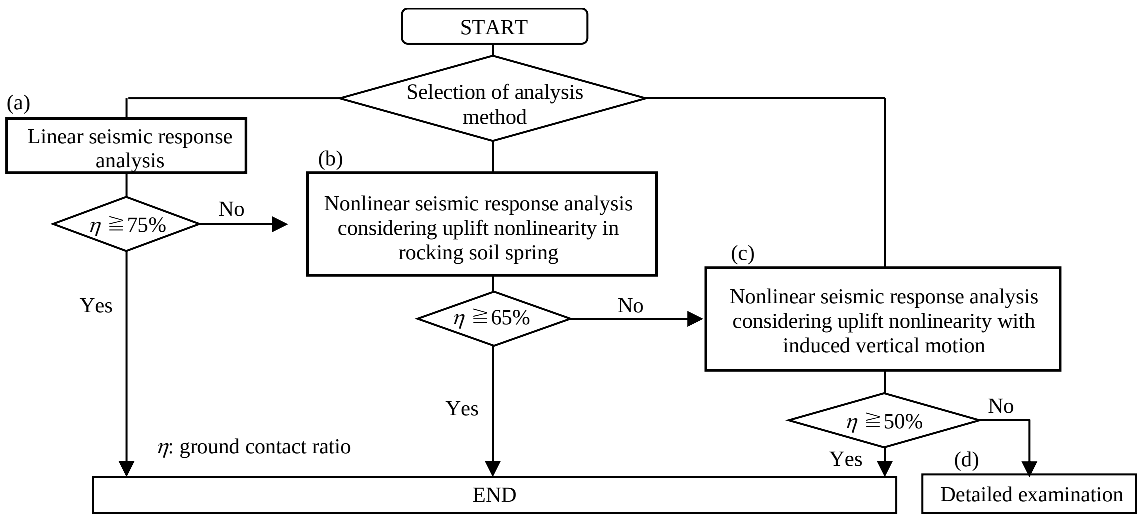

Figure 1. Evaluation procedure of basemat uplift analysis (Japan Electric Association, 2021).

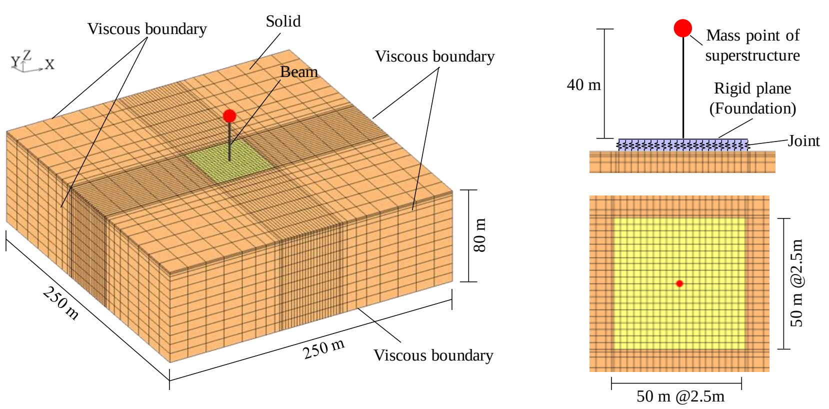

Figure 2. Aerial view of soil 3D FEM and detail of the foundation section.

OUTLINE OF THE ANALYTICAL STUDY

Overview of the FE Model

The aerial view and plane of the foundation of the 3D soil FEM under consideration are shown in Figure 2. The building was modeled using a beam element as a lumped mass system and soil as solid elements. The building and soil were modeled as linear systems, with viscous damping applied to the sides and bottom of the soil model. The basemat was modeled as a 50 m × 50 m rigid body, with the mesh divided into 20 segments in both the width and depth directions. Joint elements (e.g., Nakamura et al., 2007) were positioned at the base of the basemat to account for basemat uplift, incorporating nonlinear characteristics in both the vertical and shear directions, as shown in Figure 3. The properties of the building and soil are listed in Table 1. To investigate the impact of basemat uplift behavior in relation to the building weight and adhesion magnitude, two scenarios were considered: one with a standard weight, assuming a reactor building, and another with a lightweight, assuming an auxiliary building. The contact pressure resulting from the sustained load, calculated by dividing the total building weight by the foundation area, is also listed in Table 1. The beam element stiffness was adjusted to ensure that the first natural frequency of the building with a fixed foundation was 5 and 12 Hz in the horizontal and vertical directions, respectively, regardless of the weight. For the standard weight building, adhesion magnitudes of 0.0, 0.3, and 1.0 N/mm^2 were utilized, whereas for the lightweight building, those of 0.0, 0.1, and 0.3 N/mm^2 were employed. The building employed Rayleigh damping with a damping ratio of 5 % at reference frequencies of 5 and 50 Hz, whereas the soil employed stiffness-proportional damping of 3% at 10 Hz.

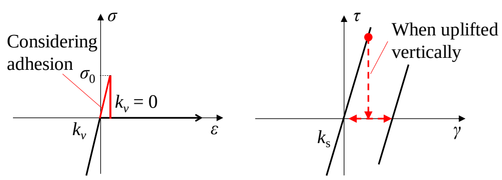

Figure 3. Nonlinearity of joint element (Left: vertical direction, Right: shear direction).

Table 1: Specifications of the building and soil

Building		Standard weight	Lightweight
Mass (t)	Superstructure	50,000	25,000
	Foundation	150,000	50,000
Ground pressure (N/mm^2)		0.78	0.29
Natural frequency (Hz)	Horizontal	5.0	
	Vertical	12.0	
Damping constant [a]		0.05	
Adhesion (N/mm^2)		0.0, 0.3, 1.0	0.0, 0.1, 0.3

[a] Rayleigh frequency to reference frequencies of f_1 = 5 Hz and f_2 = 50 Hz

soil	Soft rock	Hard rock
Shear wave velocity (m/s)	700	1500
Poisson ratio	0.35	
Density (t/m^3)	2.7	
Damping constant [b]	0.03	

[b] Stiffness-proportional frequency to the reference frequency of 10 Hz

Overview of the Simplified Method

This section presents an overview of the simplified method known as the adhesion co-considered sway rocking (SR) model, which will be compared with 3D soil FEM. The conceptual diagrams of the simplified method and the restoring force characteristics based on the moment and rotation relationship for considering basemat uplift, which will be discussed later are shown in Figure 4. In the simplified method, corresponding to the method of Figure 1 (b), an approach to model the foundation and soil as sway and rocking springs was proposed (Japan Electric Association, 2021; Tanaka et al., 2008). When considering basemat uplift, the sway spring is assumed to be linear, whereas the rocking spring incorporates nonlinear characteristics regarding the relationships between moment M, rotation angle θ, and contact ratio η, as described in Equations (1) – (4a, b) considering the adhesion effect. Notably, the vertical motion induced by basemat uplift was not considered.

$$M = M_0\left(\frac{\alpha}{2} - \frac{\alpha-2}{2}\eta\right) + M_{at}\eta^{\frac{\alpha-2}{2}} \tag{1}$$

$$M_0 = \frac{WL}{\alpha}, M_{at} = \frac{\sigma_{at}AL}{\zeta} \tag{2a, b}$$

$$\theta = \frac{\theta_0}{\eta^{\frac{\alpha-2}{2}}} + \frac{\theta_{at}}{\eta^{\left(\frac{\alpha-2}{2}\right)\frac{1}{2}}} \tag{3}$$

$$\theta_0 = M_0/K_{R0}, \theta_{at} = M_{at}/K_{R0} \tag{4a, b}$$

where M_0 represents the uplift limit moment, M_{at} represents the increase in uplift limit moment owing to adhesion, W represents the building weight, L represents the foundation width, σ_{at} represents the magnitude of adhesion, A represents the foundation bottom area, θ_0 represents the uplift limit rotation angle, θ_{at} represents the increase in uplift limit rotation angle owing to adhesion, and K_{R0} represents the linear stiffness of the rocking spring. Additionally, α and ζ are constants determined by the assumption of ground contact force distribution, where $\alpha = 4.7, \zeta = 8.6$ for rigid plate distribution, and $\alpha = \zeta = 6$ for uniform triangular distribution. The stiffness and damping coefficients of the rocking spring for seismic response analysis are expressed using Equations (5a, b). In this study, unless otherwise specified, kN is utilized as the standard unit for force and m for length.

$$K_{RR} = \frac{M}{\theta}, C_{RR} = C_{R0} \cdot \eta^{\frac{\alpha}{2}} \tag{5a, b}$$

where C_{R0} represents the damping coefficient of the rocking spring under linear conditions. The stiffness and damping coefficients in each direction for the linear condition, obtained using vibration admittance theory (Tajimi, 1959), are listed in Table 2.

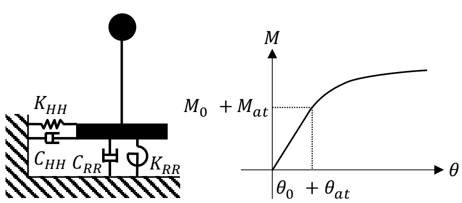

Figure 4. Conceptual diagram of the simplified method (SR model) and restoring force characteristics of the correlation of moment M and rotation angle θ.

Table 2: Specifications of soil spring

Soil	Sway spring		Rocking spring	
	K_{H0} (kN/m)	C_{H0} (kNs/m)	K_{R0} (kNm/rad)	C_{R0} (kNms/rad)
Soft rock	1.83×10^8	4.59×10^6	$1.29\text{E}\times10^{11}$	1.08×10^9
Hard rock	8.42×10^8	9.80×10^6	$5.91\text{E}\times10^{11}$	2.21×10^9

Analysis Conditions and Seismic Input Motion

Seismic response analysis was conducted as a nonlinear time-history response analysis. The analysis time step was set at 0.002 s, with time integration performed using the Newmark-β method (β = 0.25).

The time history waveform is shown in Figure 5, with a time step of 0.01 s, along with the acceleration response spectrum of the input seismic motion for analysis. The input seismic motion shown in the figure is a simulated seismic wave utilized for the bedrock in previous studies (e.g., Yamamoto et al., 2019), with a peak acceleration of 450 cm/s^2. The seismic motion is defined at the ground surface position of the free field and applied only in the horizontal direction. In the 3D soil FEM, a corrected input wave was calculated to match the seismic motion at the soil surface in the soil model, as shown in Figure 5. This wave is input through a viscous boundary at the bottom of the soil model. The seismic response analysis in this study involves multiplying the corrected input waves by coefficients to explore the relationship between adhesion and the minimum ground contact ratio resulting from basemat uplift. The maximum scaling factor for the input wave is set to cover amplitude levels that envelop a minimum ground contact ratio of 35%, considered a guideline for the applicable range of the 3D soil FEM. The duration of seismic motion was approximately 27 s.

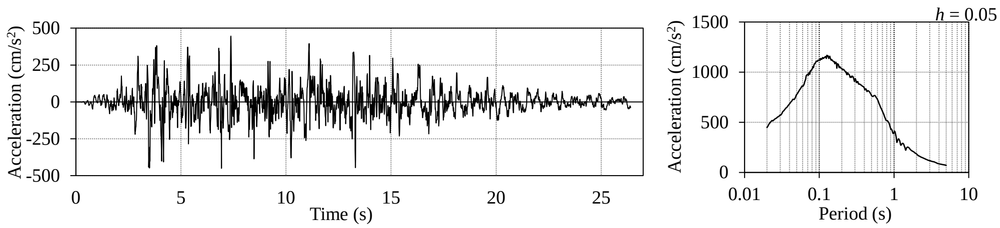

Figure 5. Input seismic motion (Left: acceleration time history, Right: acceleration response spectrum)

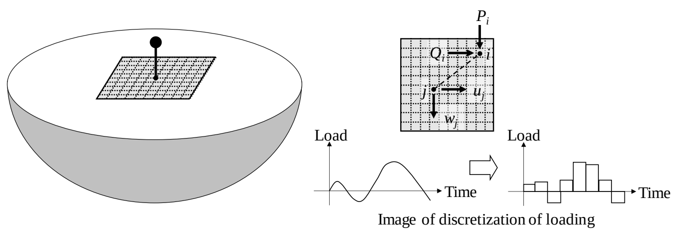

Figure 6. Conceptual diagram of the Green's function method.

ANALYSIS RESULTS

This section validates the modeling accuracy of 3D soil FEM under non-adhesive conditions by comparing it with the impulsive Greens function method (Shimomura and Tajimi, 1988, GFM). The FEM's response characteristics are compared with GFM, which treats soil as a semi-infinite medium. The conceptual diagram of the GFM is shown in Figure 6. A parametric study is conducted using 3D soil FEM, varying building weight, ground properties, and joint element adhesion magnitude. The effects of adhesion on building response characteristics are analyzed based on ground contact ratio variations during basemat uplift under different conditions.

Finally, the simplified method was evaluated by examining the relationship between moment, minimum ground contact ratio, rotation angle, and seismic responses. The results were compared with 3D soil FEM results, with each abbreviation indicating the analysis method, building weight, S-wave velocity of the soil, and adhesion. For example, a case involving 3D soil FEM with standard weight, hard rock soil, and no adhesion is denoted as FEM-SW-Vs1500-A0.0.

Validation of the Accuracy of 3D Soil FEM

Here, seismic response analyses were conducted assuming no adhesion. The analyses involve gradually increasing the amplitude of the input seismic motion for both 3D soil FEM and GFM. The purpose was to compare the responses from both methods to assess the modeling accuracy of the 3D soil FEM. For this analysis, a building with standard weight was utilized.

Comparisons between the 3D soil FEM and GFM as the input seismic motion is incrementally increased are shown in Figures 7 (a) – (c), focusing on the minimum ground contact ratio (η), as well as the response ratios (FEM/GFM) in terms of maximum horizontal acceleration response ratio (α_{SH}) and maximum vertical acceleration response ratio (α_{SV}). Notably, the response ratio for α_{SV} in Figure 7 (c) is displayed for areas in which significant vertical response occurs with ground contact ratios of approximately 65% or less. The horizontal axis in each figure represents the maximum acceleration of the seismic input motion (maximum input acceleration).

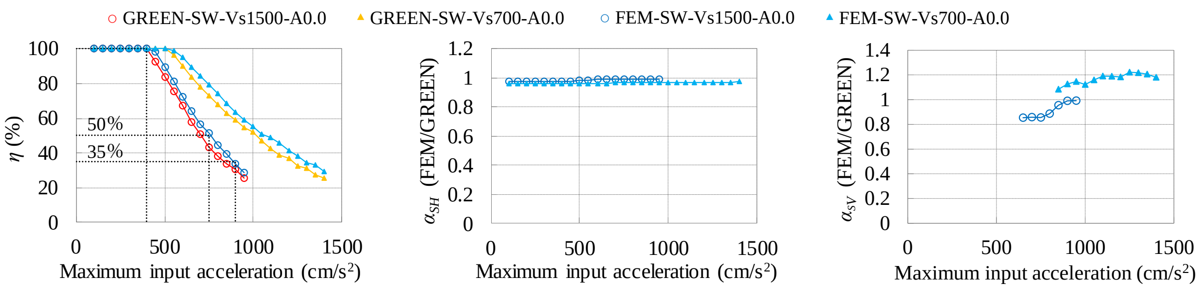

(a) η (b) α_{SH} (c) α_{SV}

Figure 7. Relationships between maximum or minimum response values and maximum input acceleration. ((a) Minimum ground contact ratio η, (b) maximum horizontal acceleration response of the superstructure α_{SH}, and (c) maximum vertical acceleration response of the superstructure α_{SV}).

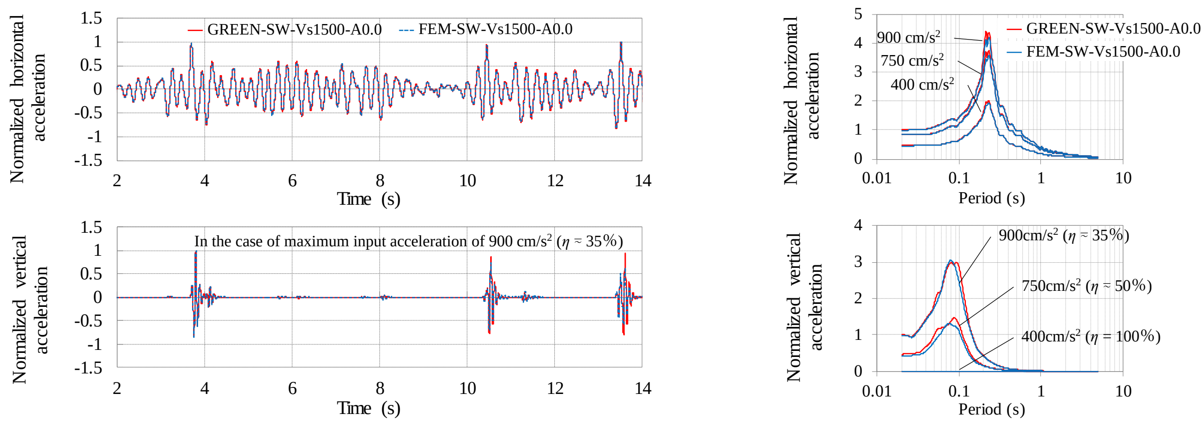

(a) Acceleration time history (b) Acceleration response spectrum

Figure 8. Acceleration time history and acceleration response spectrum (h = 0.05) of the superstructure (Top: horizontal direction, Bottom: vertical direction).

Regarding η shown in Figure 7 (a), regardless of ground conditions, the responses of both analysis methods are consistent over the entire range of input seismic motions. The relationship between the magnitude of input seismic motion and η for the case of the soft rock soil (V_S = 700 m/s) and hard rock (V_S = 1500 m/s) displays different trends. Therefore, further investigations were conducted for both soft and hard rock soil conditions for the 3D soil FEM in a later section. As shown in Figure 7 (b), α_{SH} is approximately 1.0, whereas α_{SV} is approximately 0.8 to 1.2, as shown in Figure 7 (c), indicating that the responses from 3D soil FEM analysis and GFM are generally consistent.

The acceleration time history, normalized by the maximum value of the GFM, for the duration range of 2-14 s corresponding to the minimum contact ratio η = 35% for hard rock soil conditions is shown in Figure 8 (a). This serves as a case study. The normalized acceleration response spectra of the superstructure for input seismic motions are shown in Figure 8 (b), with maximum input accelerations of 400, 750, and 900 cm/s^2. These values correspond to minimum ground contact ratios of 100%, 50%, and 35% as shown in Figure 7 (a), respectively. All vertical axes in the spectra were normalized by the amplitude value at a period of 0.02 s of the GFM in the case of a maximum input acceleration of 900 cm/s^2.

The acceleration time history and response spectra properly align for both horizontal and vertical directions.

These results confirm that the 3D soil FEM demonstrates good agreement with the GFM, a rigorous solution, thereby validating the modeling accuracy.

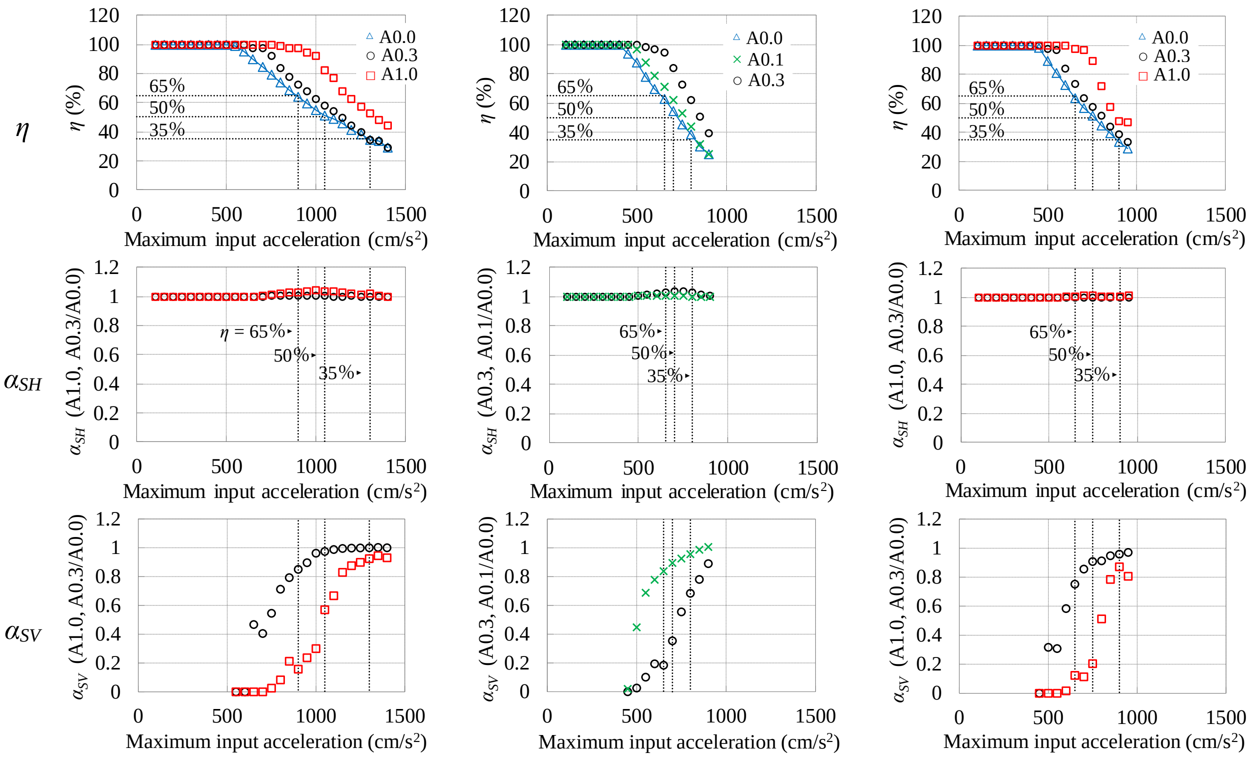

(a) FEM-SW-Vs700 (b) FEM-LW-Vs700 (c) FEM-SW-Vs1500

Figure 9. Relationships between each response value and maximum input acceleration (from top to bottom: Minimum ground contact ratio (η), maximum horizontal acceleration response of the superstructure (α_{SH}) and maximum vertical acceleration response of the superstructure (α_{SV})) when the building weight or ground properties is changed.

Effect of Adhesion on Seismic Response

A parametric study using 3D soil FEM was conducted by varying adhesion amplitudes to examine the effects of adhesion on seismic response in different building weights and ground properties. Three cases were compared: standard weight on soft rock soil, light weight on soft rock soil, and standard weight on hard rock soil.

Figures 9 (a) – (c) show comparisons of the minimum ground contact ratio (top), maximum horizontal (middle), and vertical acceleration response ratios (bottom) of the superstructure for each case when the maximum input acceleration is gradually increased. The acceleration response ratios are normalized by the response of the A0.0 case without adhesion. However, the vertical response ratio for A0.0 when ground contact ratios were 100%, was omitted because no vertical response occurred. As shown in Figures 9 (a) – (c), regardless of building weight or ground properties, when seismic motion causes minimum ground contact ratios of approximately 35% in cases without adhesion, the inclusion of adhesion increases the minimum ground contact ratio, as indicated in the top panels. The horizontal response of the building, as shown in the middle panels, exhibits minimal variation with varying degrees of adhesion. In the bottom panels, when adhesion reached a level equal to or greater than the ground contact pressure resulting from the sustained load calculated by building weight/foundation area (A1.0: adhesion is 1.0 N/mm^2 for standard weight ground contact pressure of 0.78 N/mm^2, and A0.3: adhesion is 0.3 N/mm^2 for lightweight ground contact pressure of 0.29 N/mm^2), the increase in vertical response is suppressed owing to increased ground contact ratio until a maximum input acceleration of approximately 1000 cm/s^2 is achieved. Additionally, differences in building weight result in varying degrees of increase in the minimum ground contact ratio compared with cases without adhesion, even with the same adhesion value of 0.3 N/mm^2 (Figures 9 (a) and (b)). Furthermore, the effects of adhesion were consistent across various ground properties (Figures 9 (a) and (c)).

The acceleration response spectra of the superstructure for each case are shown in Figures 10 (a) – (c), focusing on the input seismic motion where the minimum ground contact ratio was $\eta_{A0.0}$ = 50% without adhesion (refer to each plot in Figure 9 (a) for maximum input acceleration). For comparison, each figure included responses at inputs in which the minimum ground contact ratio was $\eta_{A0.0}$ = 65% for cases without adhesion. As shown in the upper figures, the horizontal responses remained consistent regardless of the level of adhesion, suggesting that the impact of adhesion on both maximum response values and spectral characteristics was minimal. Conversely, the lower figures (a) to (c) displayed a different scenario in the vertical direction. Even when subjected to input corresponding to minimum ground contact ratio $\eta_{A0.0}$ = 50% without adhesion, the cases with maximum adhesion (A1.0 for standard weight and A0.3 for lightweight) demonstrated an increase in the ground contact ratio, resulting in vertical responses lower than or equal to those of $\eta_{A0.0}$ = 65%. This trend was particularly evident in lightweight buildings (refer to the responses of blue line A0.0 and black line A0.3 in Figure 10 (b)).

These findings suggest that when adhesion was considered in 3D soil FEM, vertical responses were significantly diminished, particularly when the level of adhesion approached or exceeded the ground contact pressure caused by the building's weight. Additionally, instances in which the minimum ground contact ratio was approximately 50% without adhesion increased to 65% or higher when adhesion was considered. As shown in Figure 1 (b), when the ground contact ratio increases, seismic responses can be appropriately evaluated not only through 3D soil FEM but also through simplified methods. Therefore, it is meaningful to verify the applicable range of the simplified method.

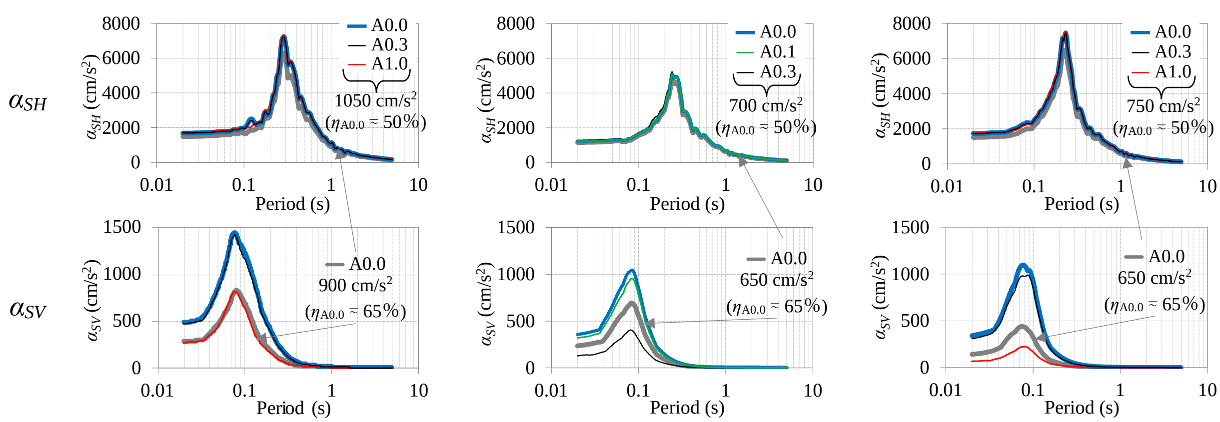

(a) FEM-SW-Vs700 (b) FEM-LW-Vs700 (b) FEM-SW-Vs1500

Figure 10. Comparison of horizontal α_{SH} and vertical acceleration response spectrum α_{SV} (h = 0.05) when the building weight or ground specifications are changed.

Rationalization of Seismic Response Analysis Utilizing the Simplified Method

The study compared 3D soil FEM analysis with simplified method to assess the applicable range of the simplified method (denoted as SR in the later figures). The study focused on horizontal response owing to the simplified method's lack of consideration for induced vertical motion. The applicable range was primarily for ground contact ratios of 65% or higher (as shown in Figure 1).

First, the relationships of moment, minimum ground contact ratio, and rotation angle based on simplified method were compared with those of the 3D soil FEM for the same three cases in the previous section. The simplified method's approximate values were calculated from Equations (1) to (4a, b). The comparison of moment and rotation angle between Figures 11 (a) to (c) reveals that the presence of adhesion increases the ground contact ratio from approximately 50% to 65% or higher. Additionally, the simplified method consistently aligned with the responses of the 3D soil FEM, even when the ground contact ratio was as low as 35%.

Comparisons of the horizontal and vertical acceleration response spectra obtained from the seismic response analyses using the 3D soil FEM and simplified method with varying magnitudes of adhesion for the two cases with different ground conditions for the standard weight are shown in Figures 12 (a) and (b). The input seismic motions utilized three levels of maximum input acceleration corresponding to the minimum ground contact ratios $\eta_{A0.0}$ of approximately 65, 50, and 35% in the 3D soil FEM without adhesion. The comparison between the two methods, as shown in figures (a) and (b), reveals a strong correspondence in terms of predominant periods and amplitudes in the horizontal responses.

Based on the comparison between 3D soil FEM and the simplified method, the simplified method can appropriately evaluate moment, ground contact ratio, and rotation angle, considering adhesion up to a minimum ground contact ratio of approximately 35% in cases without adhesion. Furthermore, seismic response analysis using the simplified method can also appropriately evaluate horizontal response, regardless of adhesion magnitude, up to a minimum contact ratio of approximately 35%.

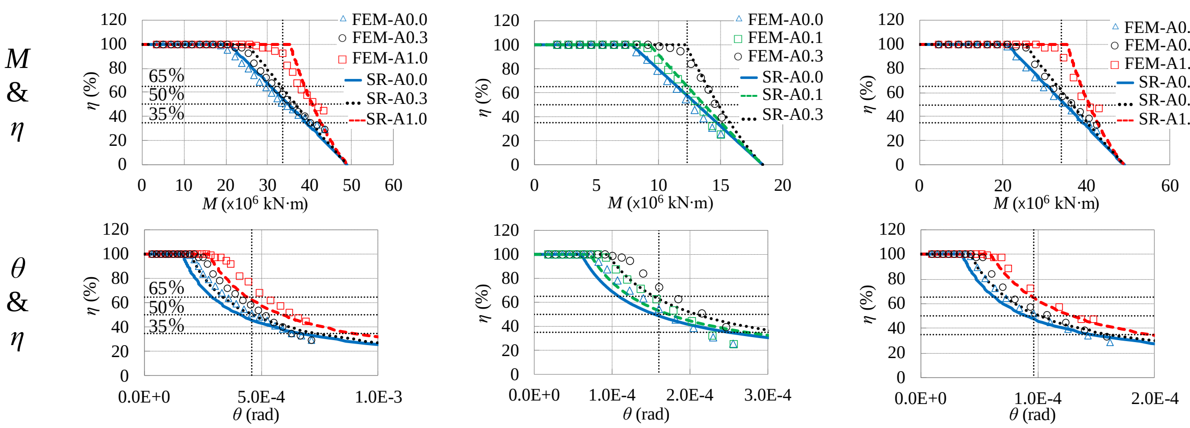

(a) SW-Vs700 (b) LW-Vs700 (c) SW-Vs1500

Figure 11. Comparison of the relationships between moment M, minimum ground contact ratio η, and rotation angle θ using FEM and SR when the building weight or ground properties vary.

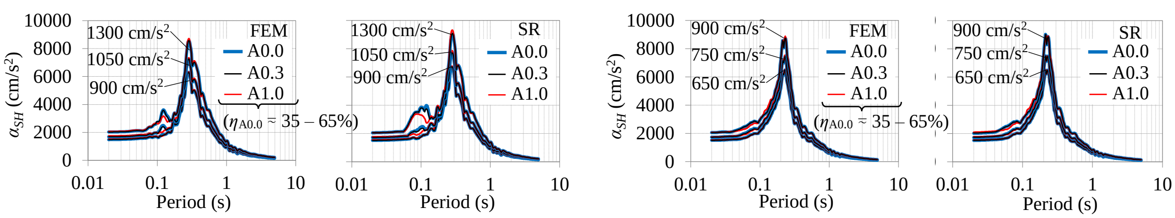

(a) SW-Vs700 (Left: FEM, Right: SR) (b) SW-Vs1500 (Left: FEM, Right: SR)

Figure 12. Comparison of horizontal acceleration response spectrum α_{SH} (h = 0.05) using FEM and the SR method when the building weight or ground properties vary.

CONCLUSIONS

Three measure conclusions can be drawn from the study.

(A) Analysis accuracy of 3D soil FEM: When the minimum ground contact ratio was approximately 35% or higher, which served as a guideline for applying the 3D soil FEM, the responses from the impulsive Green's function method (GFM), which provided rigorous analysis, and the FEM were generally consistent for both soft and hard rock soils under non-adhesion conditions. Therefore, for soft and hard rock soils with a minimum ground contact ratio of approximately 35% or higher, the analytical accuracy of the FEM can be considered reliable.

(B) Degree of adhesion contributing to seismic response suppression: When adhesion was considered in cases with 3D soil FEM, for cases with minimum ground contact ratios of approximately 35% or higher without adhesion, the minimum ground contact ratio increased when adhesion was considered. Particularly, when adhesion was comparable with the ground contact pressure owing to sustained load, the ground contact ratio increased considerably. The minimum ground contact ratio, which was approximately 50% without adhesion, was increased to over 65% when adhesion was considered, resulting in reduced vertical response.

(C) Applicable range of the simplified method (adhesion-considering SR model): Because the induced vertical motion was not considered in principle, the application range of the simplified method is for cases with a minimum ground contact ratio of 65% or higher. However, we confirmed that horizontal response and ground contact ratio were consistent with 3D soil FEM analysis down to a minimum ground contact ratio of approximately 35%. Therefore, we propose that the guideline for the application range of this method can be extended to a ground contact ratio of 35% or higher when calculating only horizontal response and ground contact ratio.

ACKNOWLEDGMENTS

This research was conducted as part of the Nuclear Risk Research Center (NRRC) Joint Research "Study on Standardization of Seismic Design and Performance Evaluation System for Nuclear Facility Buildings (Phase I)." We would like to express our gratitude to the members of the research team and the advisory committee for their valuable contributions and suggestions.

REFERENCES

Japan Electric Association (2021). “Nuclear Power Plant Seismic Design Technical Code JEAC4601-2021,” 243–267

Nakamura, N., Ino, S., Kurimoto, O. and Miake, M (2007). “An estimation method for basemat uplift behavior of nuclear power plant buildings,” *Nuclear Engineering and Design*, 237 1275–1287

Shimomura, Y., Tajimi, H. (1988). “Nonlinear Vibration Analysis of Uplifting Rigid Bodies on An Elastic Half Space,” *Procs., of Ninth World Conference of Earthquake Engineering*, Tokyo-Kyoto, 471–476.

Tajimi, H. (1959). “Basic theories on aseismic design pf structures”. Research Institute of Industrial Science and Technology, Tokyo University 8(4) 170–215 (in Japanese).

Tanaka, H., Akase, T., Omiya, Y. and Ishiguro, M. (2008). “Uplift analysis with bond stress between basemat and soil,” Summaries of Technical Papers of Annual Meeting, Architectural Institute of Japan, B-2, Structure II, 1069–1070

Tanaka, H., Tanda, H., Suzuki, T., Seko, S. and Yabushita, N. (2007). “A research on attaching forces between a bed rock and the foundation of nuclear power plant facilities (Part 1-2),” Summaries of Technical Papers of Annual Meeting, Architectural Institute of Japan, B-2, Structure II, 1073–1076

Yamamoto, S., Takada, A., Tsunashima, N., Tanaka, K., Suzuki, T., Tojo, T. and Yabushita, N. (2019). “Analytical Study of The Effect on Structure Responses of Uplift Behavior Using 3D-FE Models of reactor Buildings,” *Trans. SMiRT-25*, IASMiRT, Charlotte, NC, USA